Biochemical Journal (2017) **474** 1041–1053
DOI: 10.1042/BCJ20160990

PORTLAND PRESS

Review Article

The sleeping beauty kissed awake: new methods in electron microscopy to study cellular membranes

Petr Chlanda[1] and Jacomine Krijnse Locker[2]

[1]Eunice Kennedy Shriver National Institute of Child Health and Human Development, National Institutes of Health, 9000 Rockville Pike, Bethesda, MD 20892, U.S.A. and [2]Ultrapole, Ultra-Structural Bio-Imaging, Institut Pasteur, 28, rue du Dr. Roux, Paris 75015, France

Correspondence: Petr Chlanda (petr.chlanda@nih.gov) or Jacomine Krijnse Locker (jacomina.krijnse-locker@pasteur.fr)

Electron microscopy (EM) for biological samples, developed in the 1940–1950s, changed our conception about the architecture of eukaryotic cells. It was followed by a period where EM applied to cell biology had seemingly fallen asleep, even though new methods with important implications for modern EM were developed. Among these was the discovery that samples can be preserved by chemical fixation and most importantly by rapid freezing without the formation of crystalline ice, giving birth to the world of cryo-EM. The past 15–20 years are hallmarked by a tremendous interest in EM, driven by important technological advances. Cryo-EM, in particular, is now capable of revealing structures of proteins at a near-atomic resolution owing to improved sample preparation methods, microscopes and cameras. In this review, we focus on the challenges associated with the imaging of membranes by EM and give examples from the field of host–pathogen interactions, in particular of virus-infected cells. Despite the advantages of imaging membranes under native conditions in cryo-EM, conventional EM will remain an important complementary method, in particular if large volumes need to be imaged.

Brief history of cellular organelles imaging by electron microscopy

Much of what we know about the fundamental organization of eukaryotic cells stems from pioneering work performed in the beginning of the 20th century. The concept that cells contain structures that sediment with different densities in the centrifuge was first demonstrated by Albert Claude, who, together with his colleagues Keith Porter and Ernest Fullam, was also the first to apply electron microscopy (EM) to cultured cells ([1]; reviewed in refs [2,3]). The 'early' electron microscopists encountered challenges still valid in today's EM: how to embed samples so they can be cut into thin slices and how to create contrast in the electron microscope. Methods of sample preparation and thin sectioning, developed subsequently in the 1940–1950s, laid the ground for our current perception on intracellular membrane compartments (reviewed in ref. [2]). In fact, sample preparation by chemical fixation, heavy metal contrasting, dehydration, followed by resin embedding and sectioning is still used as a powerful and reproducible method to look inside cells.

While in the 1970–1980s EM became an important method for structural analysis of protein assemblies, EM applied to cell biology was partially left behind; the development of routines in molecular cloning enabled researchers to study the function of proteins through effects of mutations in the amino acid sequence. With commercially available light microscopes (in particular confocal microscopy) and availability of fluorescent proteins, questions related to membrane trafficking in cells were studied preferentially by light microscopy [4]. EM was considered a field carried out by a few specialists and largely made redundant by other microscopy methods. The development of cryo-EM, initiated already in the 1980s but which became routine only recently, has kissed the EM-beauty awake and rekindled an interest among researchers, including biochemists. The most recent developments in transmission EM (TEM) such as direct electron detectors, phase plate technology and novel

Received: 8 November 2016
Revised: 3 January 2017
Accepted: 23 January 2017

Version of Record published: 7 March 2017

PORTLAND PRESS

Biochemical Journal (2017) 474 1041–1053
DOI: 10.1042/BCJ20160990

methods of cell thinning allow one to study not only the structure of isolated proteins but also proteins inside cells. Furthermore, the development of scanning EM (SEM) and introduction of in-lens detectors for secondary electrons tremendously advanced the attainable resolution in SEM, which is now becoming a main technology to study large cell volumes in three dimensions.

In this review, we will highlight how these developments facilitate overcoming the main challenges in cellular EM. We will focus in particular on cellular (eukaryotic) membranes and use examples of membrane reorganization and membrane–protein interactions from the field of virus assembly and disassembly.

What are the challenges in EM applied to cell biology?

Electrons can be accelerated to such velocities that their wavelength is less than an Ångström and consequently have great resolving capabilities. However, high vacuum is needed to accelerate and focus electrons in the microscope, imposing a major constrain on biological sample imaging. A cell contains ∼70% of water, which would simply evaporate in the column of the microscope. Originally, the only way to image biological material was to remove water from cells using organic solvents whose structure was 'stabilized' by chemical fixatives and stained by heavy metals. However, all of these steps are associated with limitations; fixation, dehydration and contrasting may create artifacts. A more physiological way is to vitrify the water in cells and perform cryo-EM. The initial attempts to preserve biological samples by freezing rather than chemical fixation were clearly complicated by the high water content of such specimens; water may form ice crystals and damage the structure, making it unsuitable for ultra-structural analyses. A clear breakthrough came with the realization, previously thought impossible, that water can also form amorphous (vitreous) ice if the freezing process is fast enough. This discovery, made in parallel by Erwin Mayer and Jacques Dubochet in the 1980s, paved the way for modern cryo-EM [5,6]. However, rapid freezing at ambient pressure is limited to thin samples. Introduction of high-pressure freezing (HPF) by Moor, Mueller and colleagues allowed vitrification of samples with larger volumes such as eukaryotic cells, whole embryos or slices of a tissue [7,8]. In cryo-EM, the obvious benefits are that the samples are not chemically fixed, stained or dehydrated, and structures of organelles, macromolecules and membranes are close to their native state, immobilized in their original position within the cells.

Another big challenge of EM applied to cell biology is the thickness of the sample. In the SEM, the back-scattered or secondary electrons originating from the cell surface are analyzed, whereas in the TEM the forward-scattered electrons form the image. An important consideration is that TEM is limited to samples thinner than ∼500 nm. For thicker samples, such as whole cells, multiple electron scattering and energy loss events become too frequent to obtain an image.

Hence, in order to study cells by TEM, the cell needs to be sliced or thinned, which complicates the interpretation of cellular structures in three dimensions (3D). Tremendous efforts in the development of ultramicrotomes, diamond knives and embedding resins played a crucial role to produce sections of cells without sectioning artifacts. Recently, a complementary cell-thinning technique called focused ion beam (FIB), which is based on milling, was developed [9–12]. Both ultramicrotome automation and FIB technology combined with block-face or serial-section SEM imaging are becoming powerful methods to study membrane organelles in 3D within large biological samples [13].

Sample preservation and consequences for membranes

The very first step in classical sample preparation, fixation by aldehydes, presents a major challenge for membranes. Aldehydes bind mainly to amino groups typically contained in proteins but lacking in lipids (with some exceptions as phosphatidylserine and phosphatidylethanolamine). Proteins are cross-linked, but lipids remain mobile after fixation [14] and can be extracted by organic solvents used for subsequent dehydration. Already in the 1960s, Cope and Williams quantified extraction of various lipids species after aldehyde fixation, comparing different organic solvents and resins. Post-fixation with osmium tetroxide before dehydration reduced the extraction of lipids to different degrees, depending on the lipids species and on the resin used (reviewed in refs [15,16]). Extraction was reduced for some lipids species (e.g. cholesterol) when embedding is done at temperatures below 0°C, whereas others are extracted irrespective of the temperature (neutral lipids; [17,18]). Their study provides experimental data to support the notion that the two-step fixation, still used today, with aldehydes followed by osmium tetroxide provides a workable compromise to preserve and image membranes. Another important consideration for the preservation of lipids by EM is the choice of the buffer used for fixation (reviewed in ref. [19]); thus, phospholipids may be significantly extracted if phosphate buffers are used during fixation.

Biochemical Journal (2017) **474** 1041–1053
DOI: 10.1042/BCJ20160990

Immobilizing lipids without significant loss can be achieved only by preserving samples by vitrification where the lipids are physically rather than chemically immobilized in vitrified cells. The two most popular vitrification methods at present are plunge-freezing and HPF. For the vitrification and sample preparation by slam-freezing and freeze-etching, the reader is referred to a comprehensive review by Heuser [20]. In plunge-freezing, a thin aqueous solution of protein applied to a support for EM is plunged into a liquid nitrogen-cooled bath of ethane, obtaining cooling rates higher than 10^5 K/s [5]. This method finds its application mostly in single-particle cryo-EM to determine the structure of purified proteins, but can also be used to vitrify the peripheral regions of cells that are thinner than 5 μm [21]. To vitrify 'bigger' volumes, HPF is required. First attempts to freeze samples without ice crystal formation using high-pressure freezing were initiated in the late 1960s [22], but HPF became more routine only in 1980s. It works by applying liquid nitrogen on the sample under a pressure of 2100 bar at which free water becomes very viscous. The pressure of 2100 bar counteracts the water volume expansion, inhibiting both the nucleation and the growth of ice crystals during freezing. Hence, cooling rates required to vitrify a sample at such a pressure are two orders of magnitude lower than at ambient pressure, allowing to freeze (vitrify) considerably thicker samples (up to 200 μm) without crystals (for technical considerations, see refs [7,8,23]). With several commercially available HPF machines, it has become a common method for freezing of cells, tissues or small organisms. After HPF, samples are then further processed in two possible ways: by freeze-substitution (FS) or by direct sectioning and observation by cryo-EM. FS is performed at a low temperature, typically starting at −90°C and followed by slow gradual heating of the sample to temperatures ∼0°C. During this process, the structure of the membrane is stabilized and stained, typically using osmium tetroxide and uranyl acetate, while molecules of organic solvent slowly replace those of water present in the cell. The sample is subsequently embedded in a resin and subjected to ultramicrotomy or FIB. Compared with dehydration performed at room temperature, lipid extraction is reduced at low temperatures mainly due to slow and fixation-accompanied sample dehydration. [17,24]. Slow water–solvent exchange may also reduce osmotic pressure changes and the aggregation of proteins typically induced by chemical fixation [25]. Fixation-induced aggregation may induce proteins that are freely diffusible prior to fixation, to form an insoluble matrix. Such a matrix can then exert pulling forces on membranes inducing various artifacts such as shrinkage [26]. A typical consequence is that membranes, in particular viral membranes, are often surrounded by an 'empty' space when embedded at room temperature ([26]; see below, Figure 3A for an example).

The addition of small amounts of water [1–5% (w/w)] to the FS medium increases the contrast of membranes. This phenomenon is sample-dependent and it seems to be more pronounced at the temperatures when the osmium and uranyl acetate become reactive (between −60 and −40°C). These observations led Walther and Ziegler to propose that water creates a layer around the membranes, which improves the access of osmium and uranyl acetate to fix and stain the membranes [27,28]. HPF/FS is an excellent sample preparation technique, which provides a sufficient level of preservation to study membrane connectivity. However, an important consideration is that while osmium and uranyl acetate aid at immobilizing certain lipids, contrasting limits resolution. In essence, they create a small deposit on the structure they are bound to, limiting their resolution to roughly 2 nm [29] and preventing the analysis of fine details of membranes and associated proteins.

When it comes to structure preservation of intracellular membranes, *in situ* cryo-EM is the method of choice, and HPF/FS is a good compromise, while classical room temperature embedding suffers mostly from embedding artifacts (see ref. [26]; reviewed in ref. [30]). The obvious advantage of cryo-EM is that samples are imaged close to native conditions without dehydration and contrasting. Vitrified cells or tissues can either be sectioned in a cryo-ultramicrotome (cryo-EM of vitreous sections, CEMOVIS) or thinned in a cryo-FIB workstation maintained below the devitrification temperature (−135°C for pure water). Both techniques are technically laborious and cryo-EM imaging comes with several challenges detailed below that justify the use of room temperature EM as a complementary method. Until recently, CEMOVIS [31] was mostly perceived as a specialists' technique; however, the development of auxiliary tools (micromanipulator, charging device and improved knives) has made it more amenable to less specialized researchers [32,33]. Nevertheless, CEMOVIS is associated with limitations that relate predominantly to the sectioning process *per se*. These involve knife marks, crevasses and compression that affect cellular integrity and hence imaging. In addition, CEMOVIS is hampered by the difficulty of positioning the sections flat on the EM grid, which is problematic for cryo-electron tomography (ET; summarized in ref. [34]). Cryo-FIB is an alternative technique employing a focused ion beam to thin cells by sputtering the cellular material layer by layer in a raster manner until a 200–300 nm-thick cryo-lamella is left [35]. Compared with CEMOVIS, where cutting produces sections with compression or surface artifacts, cryo-lamellae appear artifact-free. However, cryo-FIB is a time-consuming technique since the milling speed,

Biochemical Journal (2017) **474** 1041–1053
DOI: 10.1042/BCJ20160990

determined by the current of the ion beam, is kept low to prevent sputtering artifacts. To facilitate the process of thinning, the sample can be pre-trimmed and flattened by a diamond knife (cryo-planing) prior to cryo-FIB [36,37]. The technique of cryo-FIB milling will eventually become more routine and will probably complement CEMOVIS for cell thinning, which can be further analyzed by cryo-ET [10,38,39]. For instance, CEMOVIS can produce serial sections of the cells and it is not limited only to one cryo-lamella produced from one cell.

Contrast formation in cryo-EM and recent advancements

Cryo-TEM images are noisy since biological samples are electron beam sensitive, and we can expose them only to a limited amount of electrons before their structure is damaged. Moreover, in cryo-EM, the principle of contrast formation is fundamentally different; biological macromolecules are composed of light atoms and do not absorb electrons such as in the samples stained by heavy atoms; thus, the contrast comes predominantly from phase contrast and only minimally from the absorption (amplitude) contrast [40]. To understand phase contrast, we have to remember that electrons behave as a plane wave with given amplitude and phase. The electrons interacting with biological macromolecules undergo forward scattering, changing their velocity, and the angle and length of their path on the way to the camera. Forward scattering can be either elastic or inelastic [41]. Elastically scattered electrons do not lose their kinetic energy and carry useful information about the sample. In contrast, the inelastically scattered electrons transfer part of their kinetic energy to the sample creating free radicals, causing irreversible damage to the biological structure and contributing to noise in the images. Cameras are not designed to directly detect a phase shift, but only detect differences in amplitude, which give rise to the contrast. So how do we detect phase contrast? Phase contrast results from interference of the unscattered beam with the elastically scattered electrons. Thus, phase contrast is achieved when the interference product of the incident and scattered electron waves is a wave whose amplitude difference is maximized compared with the incident electron wave. A technically feasible way to obtain phase contrast is to introduce a 90° phase shift between the incident and scattered electron wave, by modulating the focus of the objective (a phase shift of 90° comes from weak-phase object approximation and is only valid for thin samples). The phase contrast produced by defocusing is not uniform across the range of spatial frequencies and it is described by so-called contrast transfer function. Curious readers are referred to an excellent didactic review [41]. The higher the defocus, the higher is the contrast transfer of low-resolution components, allowing one to directly observe the coarse structure of the macromolecules and membranes. However, this comes at the expense of corrupting the contrast transfer at high resolution [40]. If the aim is to obtain the fine details of the structure, only a small defocus is usually applied and the contrast transfer function must be corrected. Since high-resolution frequencies are 'polluted' with noise, computational averaging techniques such as single-particle analysis [42] or sub-tomogram averaging [43] are necessary to retrieve the molecular details with sub-nanometer resolution. In summary, defocus-based phase contrast (DPC) is a common method to obtain images in cryo-EM, but it comes with a tradeoff — introducing more defocus increases contrast at the expense of high-resolution information and *vice versa*.

Already in the early development of the TEM, the idea of introducing a phase plate into the transmission electron microscope, which would produce contrast in analogy to light microscopy, came into consideration. Although several concepts have been proposed and developed, their fabrication challenges and practical disadvantages precluded their wide application. The aim of a phase plate is to achieve phase contrast, which is transferred uniformly across a broad range of spatial frequencies in close-to-focus images. This is achieved by placing a phase plate into a back-focal plane of the microscope, which introduces a desired 90° phase shift (see above) either to the unscatterred or to the scattered electron beam (for review, see ref. [44]). Recently, a self-generating, long-lasting and more user-friendly phase plate composed of a thin layer of amorphous carbon was introduced. It has been found that if the carbon is heated to ~200°C to prevent charging, electrons passing through the carbon generate Volta potential [45]. In turn, the bell-shaped Volta potential field with smooth decay introduces a phase shift to the unscattered electrons. The signal-to-noise ratio is improved in close-to-focus images compared with defocus phase contrast without compromising high-resolution spatial frequencies. Image datasets acquired with a volta-phase plate have been successfully used for averaging techniques such as single-particle analysis and sub-tomorgam averaging to obtain a protein structure with sub-nanometer resolution [46]. It has been applied to elucidate the architecture of the membrane attack complex inside the membrane induced by complement activation, which is an immune defense mechanism used against bacteria [47]. Imaging close to the focus allows direct, more accurate interpretations of membrane–protein interactions,

Biochemical Journal (2017) **474** 1041–1053
DOI: 10.1042/BCJ20160990

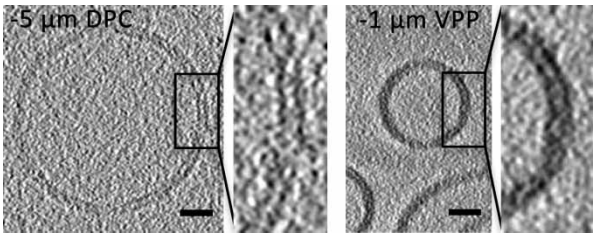

Figure 1. Comparison of defocus phase contrast (DPC) and volta-phase plate (VPP) contrast used to image a membrane.

The images show computational slices of cryo-electron tomograms of liposomes, displaying the characteristic bilayer structure of a membrane. Although the bilayer can be observed using both DPC (left) with a defocus of −5 µm and VPP (right; at a defocus of −1 µm), the contrast is higher when VPP is used. Owing to the large defocus applied in the DPC image, each monolayer of the membrane is surrounded by a low-density fringe, which may complicate direct analyses of membrane–protein interactions. Figure obtained from ref. [49].

which might be too heterogeneous for averaging methods. It can be applied to understanding organelle architecture [48], as well as influenza virus-mediated membrane fusion as shown in Figure 1 [49].

Perhaps, the most dramatic technical advancement since cryo-EM was introduced is the recent development of direct electron detectors (reviewed in ref. [50]). The detection system of a camera can be assessed by detective quantum efficiency (DQE), a ratio of the squared output and squared input signal-to-noise ratios. In other words, it refers to the added noise to the signal as a result of imperfections inherent to the detection system. DQE of the camera varies with spatial frequency, and the higher the DQE, the better. In the early days of cryo-EM, all image acquisition was done on photographic film, which was digitalized by scanning. Introduction of scintillator-coupled CCD cameras dramatically increased the throughput of imaging and enabled development of ET, albeit with lower DQE than that with photographic film. The electrons are indirectly detected in the scintillator-coupled CCD cameras: electrons hit the scintillator (phosphorus layer) and trigger a release of photons, which are focused by optical wires or lenses onto a CCD chip (reviewed in ref. [51]).

As the name indicates, direct electron detectors are capable of detecting electrons directly on a monolithic active pixel sensor circumventing the conversion to photons. Early attempts to develop such a detector were precluded by the short lifetime of the chip due to electron beam damage. The radiation hardening of the chip was achieved by so-called back-thinning of the chip, which minimizes the number of back-scattering events after the electron passes the chip on its way out of the detector. Direct detection increases the DQE by up to 80% and allows precise localization of the electrons even on a subpixel level [52]. Secondly, direct detectors are capable of fast readout (up to 400 frames/s), allowing acquisition in the movie mode, where several exposures of the same sample are made instead of one long exposure. Acquisition of multiple frames, which can be subsequently aligned and summed, allows eliminating a beam-induced drift [53]. Direct detectors fundamentally pushed the resolution limits of single-particle analysis and sub-tomogram averaging techniques to a few Ångströms [54–56].

Until recently, cryo-TEM utilizing phase contrast was only the method of choice in vitreous sample imaging. However, two studies, by Rigort et al. and by Schertel et al., showed that contrast can be obtained of unstained vitreous cells in cryo-SEM to directly observe membranous structures such as mitochondria with sufficient resolution for the 3D modeling using an in-lens secondary electron detector (Figure 2). The origin of the contrast, which depends on beam energy, is not yet fully understood. It was suggested that the contrast results from local differences in surface potential [36,57]. Another study used cryo-SEM to image the volume of high-pressure frozen sea urchin embryo and zebrafish larval tail at a resolution of 5–20 nm [58]. This technique although right now far from routine has a great potential to directly and quickly image biological samples of large volumes at native conditions.

3D Imaging of cellular membranes

EM techniques to image cells in 3D can be classified based on the type of EM such as TEM or SEM, the volume they can analyze and the resolution they can obtain. We will discuss the main 3D methods in EM (summarized in Table 1) and focus on the consequences for the imaging of membranes. There are two problems in TEM to be considered when it comes to imaging in 3D. First, as mentioned above, TEM requires the

Biochemical Journal (2017) **474** 1041–1053
DOI: 10.1042/BCJ20160990

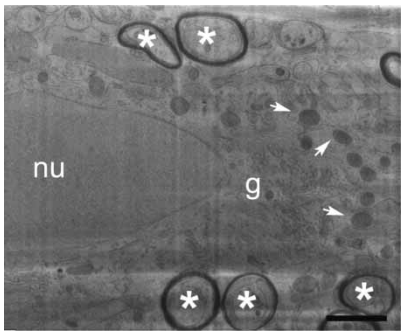

Figure 2. Cryo-FIB/SEM imaging of optic mouse nerve.

Cryo-FIB was used to mill the surface of the sample and the exposed block-face was imaged by a secondary in-lens detector. Intracellular organelles such as myelinated axons (asterisks), nucleus (nu), Golgi apparatus (g) and mitochondria (arrowheads) are clearly discernable despite the lack of any contrasting agent. Scale bars: 1 μm. Images taken from Schertel et al. [57] with permission.

inherently 3D sample to be sliced into thin sections that are approximately two-dimensional (2D) when compared with the dimensions of the cell. The second problem is that 3D intracellular structure captured within the section is projected into a 2D image. In other words, a projection TEM image is a superposition of all the structures, which interacted with the electron beam to form an image, and obviously the thicker the section of the cell, the more cellular material is projected in the image.

ET is a technique allowing to obtain 3D information of intracellular structures within a single section of the sample, which in this case is rather thick (~300 nm) to contain as much structural information as possible in the *z* direction. In ET, the sample is tilted over a range of angles with an increment of 1–3°, and at each angle a 2D projection image is acquired. The resulting tilt series of projections is subsequently aligned and back-projected *in silico* to obtain a 3D representation of structures based on the projection-slice theorem [59]. The main limitation of ET is that projections cannot be acquired at tilt angles higher than ±60–70° due to the slab geometry of the sample. Thus, although ET provides high resolution in *x*–*y* (<1 nm), the missing 40–60° of information, referred to as the missing wedge, limits the resolution in *z* [60]. ET became routine with the development of microscopes that are largely operated by software enabling them to track, focus and record

Table 1 The main three-dimensional EM imaging techniques and their applications

3D-EM technique	Application	Resolution *x*–*y* (nm)	Resolution *z* (nm)
ET	Section of sample	2	Limited by missing wedge
STEM-ET	Section of sample	5	Limited by missing wedge
SBF–SEM	Tissue	5–10	25
FIB–SEM	Whole cell	1–5	5
SS	Tissue	2	30

In ET, 200–300 nm-thick sections are tilted in the TEM (e.g. ±60°) and multiple 2D projections are recorded automatically that are computationally aligned and back-projected to obtain 3D information. STEM–ET also relies on the imaging of sections that are tilted in the TEM. Rather than recording projection images, in STEM, the sample is scanned with a beam focused into a small spot and allows for the analysis of thicker sections than in TEM–ET (see the text for an explanation). Serial block-face SEM (SBF–SEM) and focused ion beam–SEM (FIB–SEM) rely on the sample surface imaging by SEM and removing of a thin layer of material either by slicing (SBF) or by milling (FIB). By repeated cycles of slicing/milling followed by surface imaging, a 3D volume is imaged, typically a whole cell or small pieces of tissue. In SBF–SEM, a microtome is placed within the SEM, whereas in FIB–SEM an ion beam (usually composed of gallium) is used to mill the sample. Serial sectioning (SS) produces consecutive sections of defined thickness, which can be imaged either by TEM or SEM. SS–SEM is now becoming more feasible due to the development of automated microtomes and automated image acquisition in modern SEM and finds its application in the analyses of tissues. The numbers (volumes analyzed and resolution in *x*–*y* and *z*) are approximations; for details, see reviews for refs [13,39].

Biochemical Journal (2017) **474** 1041–1053
DOI: 10.1042/BCJ20160990

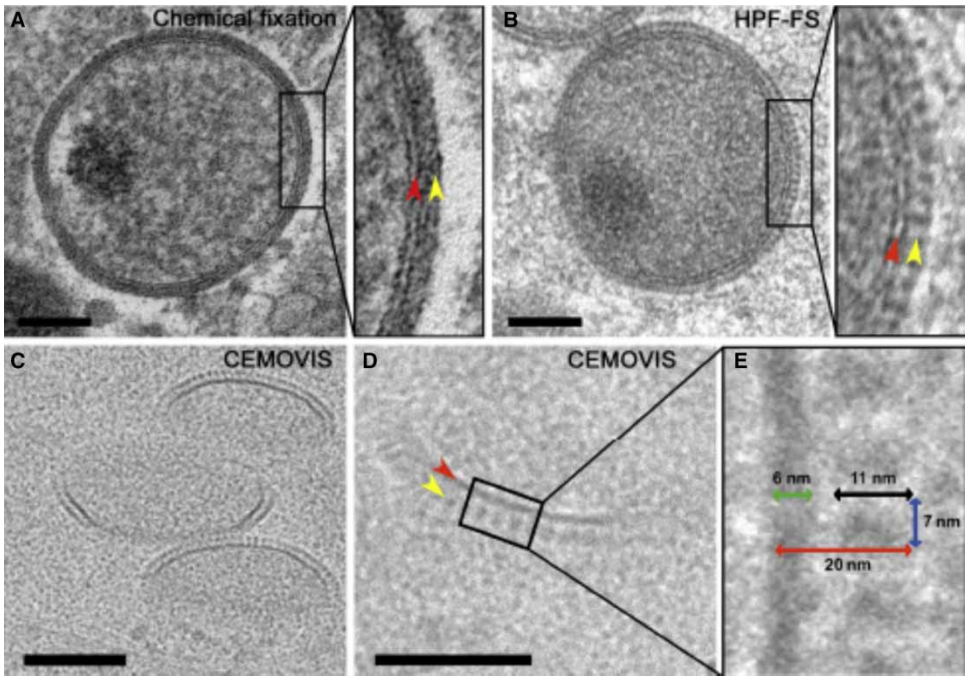

Figure 3. Comparison of the vaccinia virus membrane by different EM techniques.

The images show the immature virion and its precursor, the crescent, in thin sections of HeLa cells infected with the poxvirus vaccinia virus. Sample was (**A**) chemically fixed and embedded in epoxy resin at room temperature; (**B**) subjected to HPF, freeze-substitution and embedding at low temperature in Lowicryl; (**C**–**E**) subjected to HPF and analyzed by cryo-EM of vitreous sections (CEMOVIS). Red arrows mark a scaffold protein and yellow arrows mark a membrane. Note that the scaffold protein appears featureless after chemical fixation; after HPF/FS, the structure of the scaffold is partially revealed and CEMOVIS provides an image of the scaffold–membrane interaction under fully hydrated, native conditions and enables the measurement of the thickness of both the membrane and the scaffold. Bars: 100 nm. Taken from ref. [10], with permission of reprint.

images independently of the operator. Multiple tomograms can be acquired on serial sections with a thickness of ∼300 nm and subsequently joined, allowing one to obtain 3D information of the whole cell.

Methods relying on SEM imaging are particularly well suited for the analysis of larger volumes at a resolution determined by the minimal diameter of the focused electron beam (roughly 5 nm). SEM-based 3D methods can be further divided depending on the methods used to cut or mill the cell surface to SBF–SEM and to the above-mentioned FIB–SEM, respectively. The SBF–SEM workstation contains a built-in microtome, which removes a thin layer from the surface of the biological sample (block).

The newly exposed surface is then scanned by an electron beam focused into a probe, generating secondary or back-scattered electrons, which are detected from each spot. The whole process is repeated to image the 3D volume of the cell. FIB–SEM employs a focused ion beam (often gallium ions), which ionizes the surface and sputters the material away exposing a new surface, which is imaged by SEM. Alternatively, SEM can be used to image serial (consecutive) thin sections rather than the surface of the block. Ideally, the sections are cut as thin as possible as the resolution in z is determined by the thickness of the section (>30 nm). However, to obtain a serial section of a large biological object manually using even the most modern ultramicrotome is a tedious exercise. The recently developed Automatic Tape-collecting UltraMicrotome (ATUM) is able to automatically cut and immediately transfer thin sections of a large block on a continuous transparent tape [61]. Serial sections are subsequently imaged by SEM and can also be reanalyzed by TEM if higher resolution is required. For more details on these emerging technologies, see an excellent review by Titze and Genoud [13].

Finally, the benefits of TEM and SEM can be combined. Although less routinely used, STEM tomography is a powerful 3D EM method. Here, the sample is tilted in the microscope, identical with TEM-ET, but the electron beam is focused into a small probe that scans the sample similar to SEM. The forward-scattered

Biochemical Journal (2017) 474 1041–1053
DOI: 10.1042/BCJ20160990

(transmitted) electrons are not detected on a CCD camera but either on an axial bright-field (ABF) detector used to detect electrons scattered to low angles or high-angle annular dark-field (HAADF) detector [62]. In STEM, the objective lens is used to focus the beam into a scanning spot rather than for image formation as used in TEM. Thus, there is no objective chromatic aberration, which in classical TEM increases with sample thickness and obscures imaging of thicker samples [63]. STEM-based tomography thus allows image acquisition of samples that can be considerably thicker than in TEM-based ET (up to 1000 nm; [64,65]), permitting analyses of larger 3D volumes. For contrasted biological specimens, the ABF detector provides higher spatial resolution (5–10 nm) for 1000 nm thick samples than the HAADF detector due to a larger depth of field [66]. STEM can be performed either on TEM- or SEM-dedicated instruments equipped with a STEM detector. In some instances, STEM imaging of serial sections might be beneficial over often-used backscattered SEM imaging since it does not require heavy metal post-staining [67]. Recently, cryo-STEM was also successfully used to obtain tomograms of vitreous bacteria, illustrating the potential of this 3D imaging technique for vitreous samples [68].

Practical considerations and examples of EM methods applied to study intracellular membranes

The choice of the EM imaging technique depends on the biological question and the required resolution (which is at least 2.5 nm to resolve a 5 nm-thick membrane), sample volume to be analyzed and finally preservation level of the biological sample (discussed above). Owing to the high attainable resolution of TEM, ET is particularly well suited for studying details of the continuity of membranes in 3D (e.g. whether a vesicle is continuous or not with other cellular membrane compartments). To appreciate the overall organization of membranous organelles within cells, FIB–SEM or SBF–SEM is more appropriate than ET. For instance, to obtain a 3D image of a whole cell with an average thickness of 10 μm by ET would require joining tomograms in the *z*-axis acquired on ∼30 sections with a thickness of ∼350 nm. While possible, this is a very tedious and time-consuming exercise. Moreover, joining multiple tomograms is difficult due to uneven resin shrinkage after electron beam exposure and due to missing information as a result of lost material between sections upon each knife stroke [69]. With the 3D methods currently available, a rule of thumb is that as the volume analyzed increases, the resolution decreases. The potential resolution of 1–5 nm of SBF–SEM and FIB–SEM may at the limit to study fine details of membranes and their continuities. SBF–SEM is a method of choice when very large volumes are imaged because the built-in microtome is capable of removing material from large surfaces much faster than FIB, but the *z* resolution is lower.

Three-dimensional EM has contributed considerably to the understanding of membrane rearrangements induced by viruses. As an example, ET showed how (positive-strand) RNA viruses modify intracellular membranes utilized for the replicative cycle [70,71]. Flaviviruses such as dengue virus create invaginations of the endoplasmic reticulum, which probably facilitate genome replication while leaving a small opening through which replicated RNA can travel to the cytoplasm. ET was essential to reveal that the 11 nm-wide opening is located opposite to budding virions, indicating that replication and assembly is highly co-ordinated [72]. Other questions are addressed better using complementary 3D methods. Using a complementary set of 2D EM methods, HIV-1 was shown to bud into large, several μm-wide invaginations of the plasma membrane in primary macrophages [73]. To analyze this budding compartment in 3D, Welsch et al. [74] subsequently used serial-section ET; although powerful, the data could have been acquired faster using FIB–SEM as was subsequently shown by Bennett et al. [75] and by Höhn et al. [76]. This example nicely illustrates how fast the development of hardware in EM is currently evolving. At the time when the Welsch et al.'s (in ref. [74]) study was performed, FIB–SEM was not yet a routine, while in 2017 it clearly is.

Another example is the analysis of invaginations of the nuclear membrane induced by the human cytomegalovirus (herpesvirus) initially observed by thin-section EM [77]. Subsequent study using FIB–SEM showed how these invaginations organize into complex membrane networks devoted to virus budding [78]. Indeed, examples on how FIB–SEM contributes to, and complements, the analyses of virus-modified membrane structures are steadily increasing. They have contributed to the understanding of the architecture of the HIV-1 virological synapse [79,80]. FIB–SEM was recently also used to obtain a 3D image of Chlorella cells infected with *Paramecium bursaria chlorella virus* and was complemented with STEM–ET to image fine details of virus membrane assembly [81].

Biochemical Journal (2017) **474** 1041–1053
DOI: 10.1042/BCJ20160990

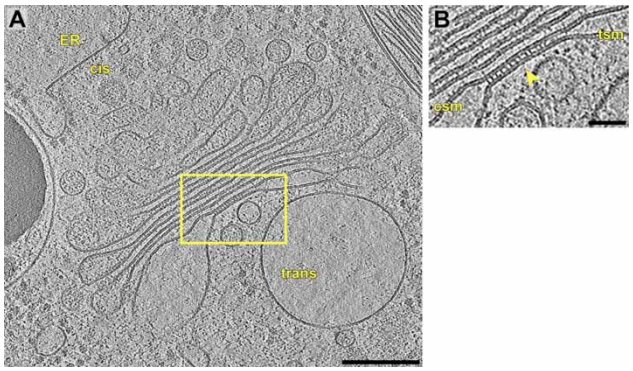

Figure 4. A slice of a cryo-electron tomogram showing a Golgi apparatus.

Chlamydomonas cells were vitrified by plunge-freezing and thinned by cryo-FIB. (**A**) Cryo-ET of vitreous cryo-lammelae shows several stacks of a Golgi apparatus without any cutting or sputtering artifacts. Scale bar: 200 nm. (**B**) A previously unidentified protein array found in the *trans*-Golgi cisternae is likely to play a role in the overall architecture of the Golgi apparatus. CSM, *cis*-membrane; TSM, *trans*-membrane. Scale bar: 50 nm. Reproduced with permission for publication by Engel et al. [86].

If the focus is on fine structure of intracellular membranes (thickness, length, curvature), including membrane–protein interactions with the possibility to retrieve high-resolution information by sub-tomogram averaging, the use of cryo-ET on samples prepared by CEMOVIS/cryo-FIB is imperative. An illustration on how conventional embedding can affect the preservation of membranes comes from the work on the poxvirus vaccinia virus (VACV). For years, the structure of its membrane was heavily debated since conventional EM suggested it to be a single bilayer with open ends in the cytoplasm, a structure never observed before in cells [82]. CEMOVIS enabled imaging the crescent-shaped precursor with unprecedented preservation: the viral membrane as a single bilayer shaped on its convex side by a scaffold protein separated by an electron-lucent space of 3 nm. The space 'disappeared' upon conventional embedding or HPF/FS and prevented the unambiguous discrimination of the different structures. Apparently dehydration resulted in the collapse of the space between the membrane and the scaffold, while the contrasting masked fine structural details and prevented the unambiguous resolution of the membrane from the scaffold [83].

However, compression and sectioning artifacts are part and parcel of CEMOVIS and have to be taken into an account when analyzing membranes. If the region of interest is in a cell periphery, which is not thicker than 300–400 nm, no sectioning is required. Thus, virus entry and exit can often be studied without sectioning. As an example cryo-ET was applied to study entry intermediates of Herpes Simplex Virus 1 (HSV1) [84] and budding of HIV-1 [85]. The recently introduced cryo-FIB offers thinning without artifacts. As an example, cryo-FIB was used to prepare a cryo-lamella of *Chlamydomonas* cells and allowed to image a Golgi apparatus without sectioning artifacts and in the native condition for the first time (Figure 4), and a protein layer responsible for stacking of the Golgi apparatus has been identified in the cisternae [86]. Thus, cryo-ET on cryo-lamella (cryo-FIB/ET) is right now the state-of-the-art technology to image intracellular membranes. This technology is directly amenable to sub-tomogram averaging and can be used to increase resolution of membrane proteins and membrane-shaping protein scaffolds inside virus-infected cells. As an example, an elegant study by Hagen et al. [87], cryo-FIB/ET was recently applied, among other methods, to study the structure of the nuclear egress coat of Herpes viruses [87].

Conclusions and perspectives

Throughout the review, we refer to the history of developments in EM since many of the 'modern' applications of EM to cell biology have been based on methods that were under continuous development for several decades. Why did the prince come along only now to kiss the sleeping beauty awake? The reasons are many and depend on countless contributions of many laboratories and companies involved in the developments. An important part of it is that modern equipment has become more user-friendly; cryo-sectioning as developed by Kiyoteru Tokuyasu [88] or by Al-Amoudi [31] used to be tedious, demanding techniques performed by only a few specialists. These can now be routinely taught to beginners owing to the development of more stable and

Biochemical Journal (2017) **474** 1041–1053
DOI: 10.1042/BCJ20160990

user-friendly microtomes. FIB technology, a relatively novel technique to thin cells, came from material sciences and was first applied in 2006; Marko et al. [11] were first to prepare a vitreous lamella of a frozen-hydrated yeast cell that was subsequently imaged by cryo-TEM. In the same year, FIB was combined with SEM to perform sequential block-face imaging of a resin-embedded whole yeast cell, critical point-dried after milling to produce a 3D image [11]. Since then a handful of laboratories have developed and improved the methodology of cryo-FIB lamella preparation [35,89,90] and protocols for FIB/SEM 3D imaging [13]. The development of software, which increased the level of automation in TEM and SEM acquisition, was the cornerstone of 3D imaging. Finally, the tremendous advancements in cryo-EM imaging for boosting the signal-to-noise ratio now enable studying the structure of proteins (particularly membrane or membrane-associated proteins that are difficult to crystalize) with near-atomic resolution [54]. Consequently, more and more biochemists are now using cryo-EM as the main method to study structure of isolated or membrane-reconstituted proteins. However, advancements in cryo-EM have not yet made their full impact on *in situ* cryo-ET studies — the future of cryo-EM lies in studying the structure of protein machineries and membranes inside the cells under close to native conditions [10]. This will allow biochemists, cell biologists and virologists to study the membrane–protein interactions at high resolution inside the cells close to their native condition.

Despite the recent developments in EM imaging, the sample preparation is still of outmost importance since poor-quality samples cannot be compensated by better microscopes or powerful software. The preservation of membranes may be of particular concern, as summarized in this review. At face value, many of the limitations associated with EM embedding can be overcome by using cryo-preservation and cryo-EM, such as artifacts of fixation, dehydration, contrasting and resin embedding. With cryo-techniques becoming more accessible owing to an increasing number of national and centralized EM facilities, it is plausible that cryo-EM will eventually replace routine protocols of chemical fixation and resin embedding to study intracellular membranes. However, some hurdles of cryo-EM will not be easily overcome: a paramount prerequisite for cellular cryo-EM is vitrification and even the most modern HPF machines cannot vitrify samples thicker than 200–300 μm due to physical properties of free water. Chemical fixation and resin embedding will thus further be necessary to study large biological volumes such as whole embryos or tissues. As mentioned already by Cope and Williams in the 1960s, it will remain important to address questions using several complementary EM techniques combined with statistical analysis to convince us that what we see is true. The hope is that the powerful capabilities of EM will continue exciting many young scientists, who in turn will come up with many more ideas for improving sample preparation and imaging techniques in EM to continue its wave of success.

Abbreviations

2D, two-dimensional; 3D, three dimensions; ABF, axial bright-field; CEMOVIS, cryo-EM of vitreous sections; DQE, detective quantum efficiency; EM, electron microscopy; ET, electron tomography; FIB, focused ion beam; FIB–SEM, focused ion beam–SEM; FS, freeze-substitution; HPF, high-pressure freezing; SBF–SEM, serial block-face SEM; SEM, scanning EM; SS, serial sectioning; TEM, transmission EM; VPP, volta-phase plate.

Acknowledgements

We thank Wiebke Moebius (MPI, Goettigen, Germany), Wolfgang Baumeister and Ben Engel (MPI, Martinsried, Germany) for permitting us to reprint their images. We are grateful to Gareth Griffiths (University of Oslo, Norway) and Martin Sachse (Institut Pasteur, Paris, France) for their critical reading of the review.

Competing Interests

The Authors declare that there are no competing interests associated with the manuscript.

References

1 Porter, K.R., Claude, A. and Fullam, E.F. (1945) A study of tissue culture cells by electron microscopy: methods and preliminary observation. *J. Exp. Med.* **81**, 233 doi:10.1084/jem.81.3.233
2 Palade, G.E. (1971) Albert claude and the beginnings of biological electron microscopy. *J. Cell Biol.* **50**, 5 doi:10.1083/jcb.50.1.5d
3 Mullock, B.M. and Luzio, J.P. (2005) Theory of organelle biogenesis: a historical perspective. In *The biogenesis of cellular organelles* (Mullins, M.C., ed.), 1–18
4 Griffiths, G., Parton, R.G., Lucocq, J., van Deurs, B., Brown, D., Slot, J.W. et al. (1993) The immunofluorescent era of membrane traffic. *Trends Cell Biol.* **3**, 214–219 doi:10.1016/0962-8924(93)90114-G
5 Mayer, E. and Brüggeller, P. (1980) Complete vitrification in pure liquid water and dilute aqueous solutions. *Nature* **288**, 569–517 doi:10.1038/288569a0

6 Dubochet, J. and McDowall, A.W. (1981) Vitrification of pure water for electron microscopy. *J. Microsc.* **124**, nRP3–RP4 doi:10.1111/j.1365-2818.1981.tb02483.x
7 Moor, H. (1987) Theory and practice of high pressure freezing. In *Cryotechniques in Biological Electron Microscopy* (Steinbrecht, R.A. and Zierold, K. eds), pp. 175–191, Springer, Berlin, Heidelberg
8 Studer, D., Michel, M. and Muller, M. (1989) High pressure freezing comes of age. *Scanning Microsc. Suppl.* **3**, 253–268; discussion 268–259 PMID:2694271
9 Heymann, J.A., Hayles, M., Gestmann, I., Giannuzzi, L.A., Lich, B. and Subramaniam, S. (2006) Site-specific 3D imaging of cells and tissues with a dual beam microscope. *J. Struct. Biol.* **155**, 63–73 doi:10.1016/j.jsb.2006.03.006
10 Mahamid, J., Pfeffer, S., Schaffer, M., Villa, E., Danev, R., Cuellar, L.K. et al. (2016) Visualizing the molecular sociology at the HeLa cell nuclear periphery. *Science* **351**, 969–972 doi:10.1126/science.aad8857
11 Marko, M., Hsieh, C., Moberlychan, W., Mannella, C.A. and Frank, J. (2006) Focused ion beam milling of vitreous water: prospects for an alternative to cryo-ultramicrotomy of frozen-hydrated biological samples. *J. Microsc.* **222**, 42–47 doi:10.1111/j.1365-2818.2006.01567.x
12 Narayan, K. and Subramaniam, S. (2015) Focused ion beams in biology. *Nat. Methods* **12**, 1021–1031 doi:10.1038/nmeth.3623
13 Titze, B. and Genoud, C. (2016) Volume scanning electron microscopy for imaging biological ultrastructure. *Biol. Cell* **108**, 307–323 PMID:27432264
14 Tanaka, K.A., Suzuki, K.G., Shirai, Y.M., Shibutani, S.T., Miyahara, M.S., Tsuboi, H. et al. (2010) Membrane molecules mobile even after chemical fixation. *Nat. Methods* **7**, 865–866 doi:10.1038/nmeth.f.314
15 Takatori, S., Mesman, R. and Fujimoto, T. (2014) Microscopic methods to observe the distribution of lipids in the cellular membrane. *Biochemistry* **53**, 639–653 doi:10.1021/bi401598v
16 Takatori, S. and Fujimoto, T. (2015) Microscopy of membrane lipids: how precisely can we define their distribution? *Essays Biochem.* **57**, 81–91 doi:10.1042/bse0570081
17 Cope, G.H. and Williams, M.A. (1968) Quantitative studies on neutral lipid preservation in electron microscopy. *J. R. Microsc. Soc.* **88**, 259–277 doi:10.1111/j.1365-2818.1968.tb00612.x
18 Cope, G.H. and Williams, M.A. (1969) Quantitative studies on the preservation of choline and ethanolamine phosphatides during tissue preparation for electron microscopy. I. Glutaraldehyde, osmium tetroxide, Araldite methods. *J. Microsc.* **90**, 31–46 doi:10.1111/j.1365-2818.1969.tb00692.x
19 Griffiths, G. (1993) *Fine Structure Immuno-Cytochemistry*, Srpinger Verlag, Heidelberg
20 Heuser, J.E. (2011) The origins and evolution of freeze-etch electron microscopy. *J. Electron. Microsc.* **60**(Suppl 1), S3–29 doi:10.1093/jmicro/dfr044
21 Medalia, O., Weber, I., Frangakis, A.S., Nicastro, D., Gerisch, G. and Baumeister, W. (2002) Macromolecular architecture in eukaryotic cells visualized by cryoelectron tomography. *Science* **298**, 1209–1213 doi:10.1126/science.1076184
22 Moor, H. and Riehle, U. (1968) Snal-freezing under high pressure: a new fixation technique for freeze-etching. *Proc. Fourth Europ. Reg. Conf. Elect. Microsc.* **2**, 33–34
23 Studer, D., Michel, M., Wohlwend, M., Hunziker, E.B. and Buschmann, M.D. (1995) Vitrification of articular cartilage by high-pressure freezing. *J. Microsc.* **179**, 321–332 doi:10.1111/j.1365-2818.1995.tb03648.x
24 Weibull, C. and Christiansson, A. (1986) Extraction of proteins and membrane lipids during low temperature embedding of biological material for electron microscopy. *J. Microsc.* **142**, 79–86 doi:10.1111/j.1365-2818.1986.tb02739.x
25 Kellenberger, E. (1991) The potential of cryofixation and freeze substitution: observations and theoretical considerations. *J. Microsc.* **161**, 183–203 doi:10.1111/j.1365-2818.1991.tb03083.x
26 Dubochet, J. and Sartori Blanc, N. (2001) The cell in absence of aggregation artifacts. *Micron* **32**, 91–99 doi:10.1016/S0968-4328(00)00026-3
27 Walther, P. and Ziegler, A. (2002) Freeze substitution of high-pressure frozen samples: the visibility of biological membranes is improved when the substitution medium contains water. *J. Microsc.* **208**, 3–10 doi:10.1046/j.1365-2818.2002.01064.x
28 Buser, C. and Walther, P. (2008) Freeze-substitution: the addition of water to polar solvents enhances the retention of structure and acts at temperatures around −60°C. *J. Microsc.* **230**, 268–277 doi:10.1111/j.1365-2818.2008.01984.x
29 Studer, D., Humbel, B.M. and Chiquet, M. (2008) Electron microscopy of high pressure frozen samples: bridging the gap between cellular ultrastructure and atomic resolution. *Histochem. Cell Biol.* **130**, 877–889 doi:10.1007/s00418-008-0500-1
30 Mielanczyk, L., Matysiak, N., Michalski, M., Buldak, R. and Wojnicz, R. (2014) Closer to the native state. Critical evaluation of cryo-techniques for transmission electron microscopy: preparation of biological samples. *Folia Histochem. Cytobiol.* **52**, 1–17 doi:10.5603/FHC.2014.0001
31 Al-Amoudi, A., Chang, J.-J., Leforestier, A., McDowall, A., Salamin, L.M., Norlén, L.P.O. et al. (2004) Cryo-electron microscopy of vitreous sections. *EMBO J.* **23**, 3583–3588 doi:10.1038/sj.emboj.7600366
32 Pierson, J., Fernández, J.J., Bos, E., Amini, S., Gnaegi, H., Vos, M. et al. (2010) Improving the technique of vitreous cryo-sectioning for cryo-electron tomography: electrostatic charging for section attachment and implementation of an anti-contamination glove box. *J. Struct. Biol.* **169**, 219–225 doi:10.1016/j.jsb.2009.10.001
33 Studer, D., Klein, A., Iacovache, I., Gnaegi, H. and Zuber, B. (2014) A new tool based on two micromanipulators facilitates the handling of ultrathin cryosection ribbons. *J. Struct. Biol.* **185**, 125–128 doi:10.1016/j.jsb.2013.11.005
34 Hurbain, I. and Sachse, M. (2011) The future is cold: cryo-preparation methods for transmission electron microscopy of cells. *Biol. Cell* **103**, 405–420 doi:10.1042/BC20110015
35 Schaffer, M., Mahamid, J., Engel, B.D., Laugks, T., Baumeister, W. and Plitzko, J.M. (2016) Optimized cryo-focused ion beam sample preparation aimed at in situ structural studies of membrane proteins. *J. Struct. Biol.* **197**, 73–82 doi:10.1016/j.jsb.2016.07.010
36 Rigort, A., Bäuerlein, F.J.B., Leis, A., Gruska, M., Hoffmann, C., Laugks, T. et al. (2010) Micromachining tools and correlative approaches for cellular cryo-electron tomography. *J. Struct. Biol.* **172**, 169–179 doi:10.1016/j.jsb.2010.02.011
37 Walther, P. and Muller, M. (1999) Biological ultrastructure as revealed by high resolution cryo-SEM of block faces after cryo-sectioning. *J. Microsc.* **196**, 279–287 doi:10.1046/j.1365-2818.1999.00595.x
38 Rigort, A. and Plitzko, J.M. (2015) Cryo-focused-ion-beam applications in structural biology. *Arch. Biochem. Biophys.* **581**, 122–130 doi:10.1016/j.abb.2015.02.009
39 Kizilyaprak, C., Daraspe, J. and Humbel, B.M. (2014) Focused ion beam scanning electron microscopy in biology. *J. Microsc.* **254**, 109–114 doi:10.1111/jmi.12127

Biochemical Journal (2017) **474** 1041–1053
DOI: 10.1042/BCJ20160990

40 Glaeser, R.M. (2013) Invited review article: Methods for imaging weak-phase objects in electron microscopy. *Rev. Sci. Instrum.* **84**, 111101 doi:10.1063/1.4830355
41 Orlova, E.V. and Saibil, H.R. (2011) Structural analysis of macromolecular assemblies by electron microscopy. *Chem. Rev.* **111**, 7710–7748 doi:10.1021/cr100353t
42 Cheng, Y., Grigorieff, N., Penczek, P.A. and Walz, T. (2015) A primer to single-particle cryo-electron microscopy. *Cell* **161**, 438–449 doi:10.1016/j.cell.2015.03.050
43 Wan, W. and Briggs, J.A.G. (2016) Cryo-electron tomography and subtomogram averaging. *Methods Enzymol.* **579**, 329–367 doi:10.1016/bs.mie.2016.04.014
44 Danev, R. and Nagayama, K. (2010) Phase plates for transmission electron microscopy. *Methods Enzymol.* **481**, 343–369 doi:10.1016/S0076-6879(10)81014-6
45 Danev, R., Buijsse, B., Khoshouei, M., Plitzko, J.M. and Baumeister, W. (2014) Volta potential phase plate for in-focus phase contrast transmission electron microscopy. *Proc. Natl Acad. Sci. U.S.A.* **111**, 15635–15640 doi:10.1073/pnas.1418377111
46 Danev, R. and Baumeister, W. (2016) Cryo-EM single particle analysis with the Volta phase plate. *eLife* **5**, doi:10.7554/eLife.13046
47 Sharp, T.H., Koster, A.J. and Gros, P. (2016) Heterogeneous MAC initiator and pore structures in a lipid bilayer by phase-plate cryo-electron tomography. *Cell Rep.* **15**, 1–8 doi:10.1016/j.celrep.2016.03.002
48 Fukuda, Y., Laugks, U., Lučić, V., Baumeister, W. and Danev, R. (2015) Electron cryotomography of vitrified cells with a Volta phase plate. *J. Struct. Biol.* **190**, 143–154 doi:10.1016/j.jsb.2015.03.004
49 Chlanda, P., Mekhedov, E., Waters, H., Schwartz, C.L., Fischer, E.R., Ryham, R.J. et al. (2016) The hemifusion structure induced by influenza virus haemagglutinin is determined by physical properties of the target membranes. *Nat. Microbiol.* **1**, 16050 doi:10.1038/nmicrobiol.2016.50
50 McMullan, G., Faruqi, A.R. and Henderson, R. (2016) Chapter One — direct electron detectors. *Methods Enzymol.* **579**, 1–17 doi:10.1016/bs.mie.2016.05.056
51 Orlov, I., Myasnikov, A.G., Andronov, L., Natchiar, S.K., Khatter, H., Beinsteiner, B., et al. (2016) The integrative role of cryo-electron microscopy in molecular and cellular structural biology. *Biol. Cell* PMID:27730650
52 Li, X., Mooney, P., Zheng, S., Booth, C.R., Braunfeld, M.B., Gubbens, S. et al. (2013) Electron counting and beam-induced motion correction enable near-atomic-resolution single-particle cryo-EM. *Nat. Methods* **10**, 584–590 doi:10.1038/nmeth.2472
53 Li, X., Zheng, S.Q., Egami, K., Agard, D.A. and Cheng, Y. (2013) Influence of electron dose rate on electron counting images recorded with the K2 camera. *J. Struct. Biol.* **184**, 251–260 doi:10.1016/j.jsb.2013.08.005
54 Bai, X.-C., McMullan, G. and Scheres, S.H. (2015) How cryo-EM is revolutionizing structural biology. *Trends Biochem. Sci.* **40**, 49–57 doi:10.1016/j.tibs.2014.10.005
55 Bartesaghi, A., Merk, A., Banerjee, S., Matthies, D., Wu, X., Milne, J.L.S. et al. (2015) 2.2 a resolution cryo-EM structure of β-galactosidase in complex with a cell-permeant inhibitor. *Science* **348**, 1147–1151 doi:10.1126/science.aab1576
56 Schur, F.K., Obr, M., Hagen, W.J., Wan, W., Jakobi, A.J., Kirkpatrick, J.M. et al. (2016) An atomic model of HIV-1 capsid-SP1 reveals structures regulating assembly and maturation. *Science* **353**, 506–508 doi:10.1126/science.aaf9620
57 Schertel, A., Snaidero, N., Han, H.-M., Ruhwedel, T., Laue, M., Grabenbauer, M. et al. (2013) Cryo FIB-SEM: volume imaging of cellular ultrastructure in native frozen specimens. *J. Struct. Biol.* **184**, 355–360 doi:10.1016/j.jsb.2013.09.024
58 Vidavsky, N., Akiva, A., Kaplan-Ashiri, I., Rechav, K., Addadi, L., Weiner, S. et al. (2016) Cryo-FIB-SEM serial milling and block face imaging: Large volume structural analysis of biological tissues preserved close to their native state. *J. Struct. Biol.* **196**, 487–495 doi:10.1016/j.jsb.2016.09.016
59 De Rosier, D.J. and Klug, A. (1968) Reconstruction of three dimensional structures from electron micrographs. *Nature* **217**, 130–134 doi:10.1038/217130a0
60 Lučić, V., Förster, F. and Baumeister, W. (2005) Structural studies by electron tomography: from cells to molecules. *Annu. Rev. Biochem.* **74**, 833–865 doi:10.1146/annurev.biochem.73.011303.074112
61 Hayworth, K.J., Morgan, J.L., Schalek, R., Berger, D.R., Hildebrand, D.G.C. and Lichtman, J.W. (2014) Imaging ATUM ultrathin section libraries with WaferMapper: a multi-scale approach to EM reconstruction of neural circuits. *Front Neural Circuits* **8**, 68 doi:10.3389/fncir.2014.00068
62 MacArthur, K.E. (2016) The use of annular dark-field scanning transmission electron microscopy for quantitative characterization. *Johnson Matthey Technol. Rev.* **60**, 117–131 doi:10.1595/205651316X691186
63 Sousa, A.A., Azari, A.A., Zhang, G. and Leapman, R.D. (2011) Dual-axis electron tomography of biological specimens: extending the limits of specimen thickness with bright-field STEM imaging. *J. Struct. Biol.* **174**, 107–114 doi:10.1016/j.jsb.2010.10.017
64 Aoyama, K., Takagi, T., Hirase, A. and Miyazawa, A. (2008) STEM tomography for thick biological specimens. *Ultramicroscopy* **109**, 70–80 doi:10.1016/j.ultramic.2008.08.005
65 Walther, P., Schmid, E. and Höhn, K. (2013) High-pressure freezing for scanning transmission electron tomography analysis of cellular organelles. *Methods Mol. Biol.* **931**, 525–535 doi:10.1007/978-1-62703-056-4_28
66 Hohmann-Marriott, M.F., Sousa, A.A., Azari, A.A., Glushakova, S., Zhang, G., Zimmerberg, J. et al. (2009) Nanoscale 3D cellular imaging by axial scanning transmission electron tomography. *Nat. Methods* **6**, 729–731 doi:10.1038/nmeth.1367
67 Kuipers, J., de Boer, P. and Giepmans, B.N. (2015) Scanning EM of non-heavy metal stained biosamples: large-field of view, high contrast and highly efficient immunolabeling. *Exp. Cell Res.* **337**, 202–207 doi:10.1016/j.yexcr.2015.07.012
68 Wolf, S.G., Houben, L. and Elbaum, M. (2014) Cryo-scanning transmission electron tomography of vitrified cells. *Nat. Methods* **11**, 423–428 doi:10.1038/nmeth.2842
69 Höög, J.L. and Antony, C. (2007) Whole-cell investigation of microtubule cytoskeleton architecture by electron tomography. *Methods Cell Biol.* **79**, 145–167 doi:10.1016/S0091-679X(06)79006-9
70 Risco, C., de Castro, I.F., Sanz-Sánchez, L., Narayan, K., Grandinetti, G. and Subramaniam, S. (2014) Three-dimensional imaging of viral infections. *Annu. Rev. Virol.* **1**, 453–473 doi:10.1146/annurev-virology-031413-085351
71 Romero-Brey, I. and Bartenschlager, R. (2015) Viral infection at high magnification: 3D electron microscopy methods to analyze the architecture of infected cells. *Viruses* **7**, 6316–6345 doi:10.3390/v7122940

72 Welsch, S., Miller, S., Romero-Brey, I., Merz, A., Bleck, C.K.E., Walther, P. et al. (2009) Composition and three-dimensional architecture of the dengue virus replication and assembly sites. *Cell Host Microbe* **5**, 365–375 doi:10.1016/j.chom.2009.03.007
73 Welsch, S., Keppler, O.T., Habermann, A., Allespach, I., Krijnse-Locker, J. and Kräusslich, H.-G. (2007) HIV-1 buds predominantly at the plasma membrane of primary human macrophages. *PLoS Pathog.* **3**, e36 doi:10.1371/journal.ppat.0030036
74 Welsch, S., Groot, F., Krausslich, H.-G., Keppler, O.T. and Sattentau, Q.J. (2011) Architecture and regulation of the HIV-1 assembly and holding compartment in macrophages. *J. Virol.* **85**, 7922–7927 doi:10.1128/JVI.00834-11
75 Bennett, A.E., Narayan, K., Shi, D., Hartnell, L.M., Gousset, K., He, H. et al. (2009) Ion-abrasion scanning electron microscopy reveals surface-connected tubular conduits in HIV-infected macrophages. *PLoS Pathog.* **5**, e1000591 doi:10.1371/journal.ppat.1000591
76 Höhn, K., Fuchs, J., Fröber, A., Kirmse, R., Glass, B., Anders-Össwein, M. et al. (2015) Preservation of protein fluorescence in embedded human dendritic cells for targeted 3D light and electron microscopy. *J. Microsc.* **259**, 121–128 doi:10.1111/jmi.12230
77 Buser, C., Walther, P., Mertens, T. and Michel, D. (2007) Cytomegalovirus primary envelopment occurs at large infoldings of the inner nuclear membrane. *J. Virol.* **81**, 3042–3048 doi:10.1128/JVI.01564-06
78 Villinger, C., Neusser, G., Kranz, C., Walther, P. and Mertens, T. (2015) 3D analysis of HCMV induced-nuclear membrane structures by FIB/SEM tomography: insight into an unprecedented membrane morphology. *Viruses* **7**, 5686–5704 doi:10.3390/v7112900
79 Do, T., Murphy, G., Earl, L.A., Del Prete, G.Q., Grandinetti, G., Li, G.-H. et al. (2014) Three-dimensional imaging of HIV-1 virological synapses reveals membrane architectures involved in virus transmission. *J. Virol.* **88**, 10327–10339 doi:10.1128/JVI.00788-14
80 Felts, R.L., Narayan, K., Estes, J.D., Shi, D., Trubey, C.M., Fu, J. et al. (2010) 3D visualization of HIV transfer at the virological synapse between dendritic cells and T cells. *Proc. Natl Acad. Sci. U.S.A.* **107**, 13336–13341 doi:10.1073/pnas.1003040107
81 Milrot, E., Mutsafi, Y., Fridmann-Sirkis, Y., Shimoni, E., Rechav, K., Gurnon, J.R. et al. (2016) Virus-host interactions: insights from the replication cycle of the large *Paramecium bursaria chlorella virus*. *Cell. Microbiol.* **18**, 3–16 doi:10.1111/cmi.12486
82 Dales, S. and Mosbach, E.H. (1968) Vaccinia as a model for membrane biogenesis. *Virology* **35**, 564–583 doi:10.1016/0042-6822(68)90286-9
83 Chlanda, P., Carbajal, M.A., Cyrklaff, M., Griffiths, G. and Krijnse-Locker, J. (2009) Membrane rupture generates single open membrane sheets during vaccinia virus assembly. *Cell Host Microbe* **6**, 81–90 doi:10.1016/j.chom.2009.05.021
84 Maurer, U.E., Sodeik, B. and Grunewald, K. (2008) Native 3D intermediates of membrane fusion in herpes simplex virus 1 entry. *Proc. Natl Acad. Sci. U.S.A.* **105**, 10559–10564 doi:10.1073/pnas.0801674105
85 Carlson, L.-A., de Marco, A., Oberwinkler, H., Habermann, A., Briggs, J.A., Kräusslich, H.-G. et al. (2010) Cryo-electron tomography of native HIV-1 budding sites. *PLoS Pathog.* **6**, e1001173 doi:10.1371/journal.ppat.1001173
86 Engel, B.D., Schaffer, M., Albert, S., Asano, S., Plitzko, J.M. and Baumeister, W. (2015) In situ structural analysis of Golgi intracisternal protein arrays. *Proc. Natl. Acad. Sci. U.S.A.* **112**, 11264–11269 doi:10.1073/pnas.1515337112
87 Hagen, C., Dent, K.C., Zeev-Ben-Mordehai, T., Grange, M., Bosse, J.B., Whittle, C. et al. (2015) Structural basis of vesicle formation at the inner nuclear membrane. *Cell* **163**, 1692–1701 doi:10.1016/j.cell.2015.11.029
88 Griffiths, G., Slot, J.-W. and Webster, P. (2015) Kiyoteru Tokuyasu: a pioneer of cryo-ultramicrotomy. *Microscopy* **64**, 377–379 doi:10.1093/jmicro/dfv351
89 Zhang, J., Ji, G., Huang, X., Xu, W. and Sun, F. (2016) An improved cryo-FIB method for fabrication of frozen hydrated lamella. *J. Struct. Biol.* **194**, 218–223 doi:10.1016/j.jsb.2016.02.013
90 Harapin, J., Börmel, M., Sapra, K.T., Brunner, D., Kaech, A. and Medalia, O. (2015) Structural analysis of multicellular organisms with cryo-electron tomography. *Nat. Methods* **12**, 634–636 doi:10.1038/nmeth.3401